EXTENDED INTERPOLATION IN FINITE ELEMENT ANALYSIS*

L. S. D. Morley**
Royal Aircraft Establishment, Farnborough, UK

June 1971

It is a widely held view that mid-side connection properties impose a disproportionately severe penalty upon the computational efficiency of finite element calculations. Here, an exploration is made of a technique which eliminates these undesirable connections by an extension of spacewise interpolation across the boundaries of triangular finite elements and yet retains much of the original accuracy. The technique is applied with success to the conforming plate bending finite element with cubically varying normal displacement along the triangle sides and also to the plane stress element with quadratically varying displacements. An important development is a constant bending moment finite element which has the simplest possible connection properties involving only the normal displacement at the vertices of the triangle.

** Senior Principal Scientific Officer, Structures Department.

1. INTRODUCTION

The finite element method is a piecewise application of the classical Rayleigh-Ritz technique whereby all the essential connection properties between elements are determined by the governing variational principle, e.g. minimum potential or complementary energy. Spacewise interpolation techniques are employed within each element in order to set up coordinate, or shape, functions as a preliminary to the actual calculation of the numerical values associated with the connection properties. The question does not seem to have been explored, however, as to whether there may be advantages in extending these spacewise interpolation techniques across and beyond the element boundaries.

Let us begin by looking at the conforming plate bending triangular finite element with normal displacements w which vary cubically along the element sides; early formulations are given by Clough and Tocher[1] and by Bazeley *et al*[2] although a more recent formulation[3] is used for the numerical work in the present paper. The mid-side connection property, which is required to ensure continuity of the normal derivative $\partial w/\partial n$ of the displacement across the element interface, is eliminated in these early formulations as the arithmetic mean of the appropriate directional derivatives taken at the nodes at each end of the side. This simple interpolation, used with this element, leads to an unduly overstiff structure and, accordingly, finds little favour in practical applications. On the other hand, while retention of the mid-side connection leads to very satisfactory numerical results, the accompanying inflation of the computer storage requirements coupled with an increase in execution time imposes a disproportionately severe penalty upon the computational efficiency. The trivial case which is shown in Figs.1a and 1b provides an example where the storage requirement, when it is exemplified by the global stiffness matrix in banded form without sub-structuring, turns out to be doubled. Although the size of the global stiffness matrix provides an inadequate measure for the efficiency of modern computing techniques it is, nevertheless, this kind of penalty which encourages the development of higher degree elements, see, e.g. Bell[4], with excess nodal continuities but where the mid-side connection quantities are easily eliminated at element level and without significant loss of accuracy.

In re-examining the conforming plate bending triangular finite element with w displacements which vary cubically along the element sides it was noticed that it is a relatively simple matter to arrange an extension of the finite element spacewise interpolation process so as to estimate the mid-side normal derivative $\partial w/\partial n$ more accurately than hitherto. This is achieved in explicit terms of the twelve nodal connection quantities of the two triangular elements which share the common side; it produces, for example, the situation shown in Fig.1c where the size of the global stiffness matrix is only twenty per cent above that which is required for the simple interpolation of Fig.1b. Moreover, the numerical results which are calculated for the classical comparative problems of the bending of a square plate now show a negligible difference from those obtained with retention of the mid-side connection.

With this encouragement, the idea of an extended interpolation is pursued to develop a triangular plate bending element which has the simplest possible connection properties involving only the displacement w at the nodes. This development is centred around the constant bending moment element which has attracted many different derivations of what is really a strict equilibrium element, e.g.[5,6,7,8,9]. Recent derivations[8,9] are by

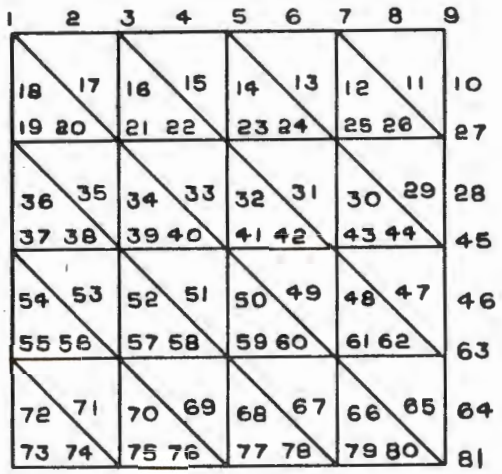

Fig.1a Mid-side connection points retained

Size of global stiffness matrix:
Rows=131
Semi-bandwidth=35
(131×35 = 4585)

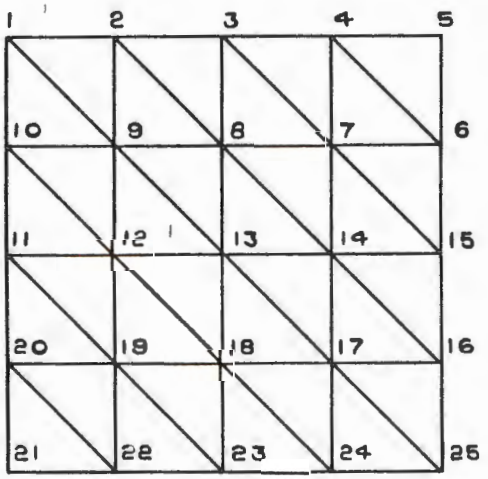

Fig.1b Mid-side connection points eliminated by simple interpolation

Size of global stiffness matrix:
Rows = 75
Semi-bandwidth = 30
(75×30 = 2250)

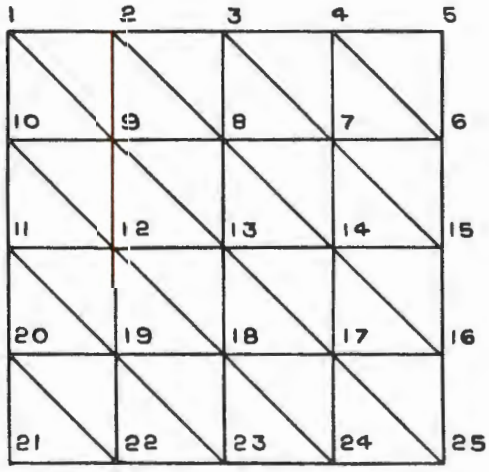

Fig. 1c Mid-side connection points eliminated by extended interpolation

Size of global stiffness matrix:
Rows = 75
Semi-bandwidth = 36
(75×36=2700)

Fig.1 Element numbering for conforming plate bending triangular elements with cubically varying edge displacement w

way of a straightforward application of the theorem of minimum potential energy to a non-conforming quadratically varying w displacement with inter-element connections of w at each node and of $\partial w/\partial n$ at each mid-side as is shown in Fig.2a. Extended interpolation is now applied to express the mid-side $\partial w/\partial n$ in terms of the displacement w at nearby nodes. Although the interpolation destroys the strict equilibrium nature of this element our numerical examples show that it provides, more often than not, agreeable improvements in the accuracy of the interesting physical quantities as is compared with the situation where the mid-side connection points are retained. One explanation for this phenomenon is that the excess flexibility of the strict equilibrium element is suitably moderated by the kinematic constraint which is imposed by the extended interpolation.

The concluding application deals with the elimination of the mid-side connection properties which are normally required for the quadratically varying displacements u and v in the well known triangular plane stress finite element[10,11]. Comparative numerical results are given here for the square plate under uniform tension which contains a central circular hole. This problem is known[12,13] to be particularly sensitive because of the severe gradients which occur in the circumferential stress resultant near the hole boundary and, indeed, the comparative finite element results for linearly varying u,v displacements are found to be virtually worthless for the mesh under investigation.

The Appendix provides a listing of a Fortran subroutine which deals rudimentarily with the topological exercise of finding, for each triangular element, those nearby node numbers which are prerequisite to the application of the extended interpolation processes.

It is emphasized that this investigation is by nature exploratory. While extended interpolation is seen to reduce the size of the overall computational problem when it is measured by the global stiffness matrix, it does involve additional computational effort at element level and, in this respect, it bears resemblance with the sub-structuring technique. Notwithstanding, the extended interpolation is likely to enjoy particularly beneficial application to studies which concern buckling, vibration and optimum design. The stratagem in the elimination of the mid-side connection quantities hinges here upon an exact recovery of all global regular polynomial solutions as are permitted by the basic shape functions of the element itself. Finally, the application of extended interpolation is most ideally suited to an element mesh of equilateral triangles although it is by no means necessary, as is evidenced by the numerical examples treated herein, to impose such a limitation on a mesh which is already in accord with sound finite element practice.

Acknowledgement is gladly given to B. C. Merrifield and to D. R. Blackeby for unstinting labours in preparing computer programs, respectively for the plate bending and for the plane stress problems, also to Carol Hanson who assisted in the preparation of the subroutine which is listed in the Appendix.

2. PLATE BENDING ELEMENT WITH CUBICALLY VARYING w-DISPLACEMENT ALONG THE SIDES

The triangular finite element of arbitrary shape is shown in Fig.3 with nodes numbered 1 3 5. A point within the element is located in the usual way by non-dimensional area coordinates L_1, L_3 and L_5 where

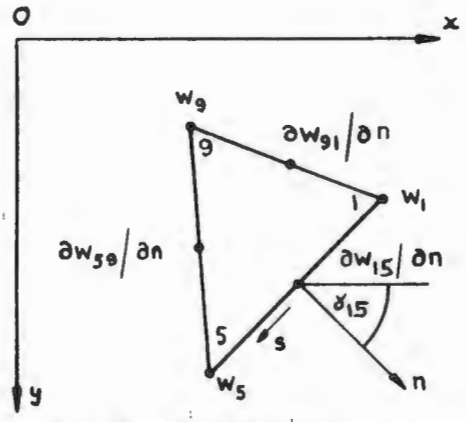

Fig. 2a Equilibrium element

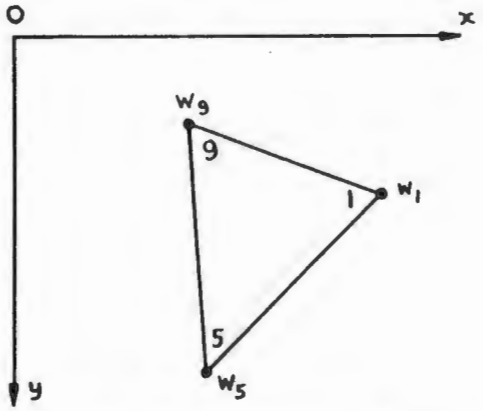

Fig. 2b With extended interpolation

Fig. 2 Connection properties of plate bending element with quadratically varying w displacement

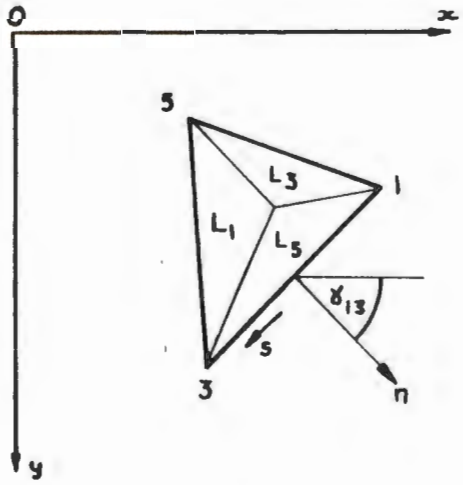

Fig. 3a Notation

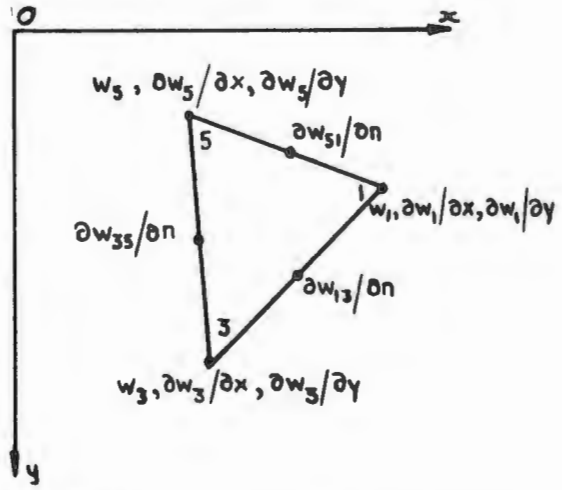

Fig. 3b Usual connection properties

Fig. 3 Plate bending element with cubically varying w displacement along the sides

$$L_1 = (a_1 + b_1 x + c_1 y)/2A,$$

$$a_1 = x_3 y_5 - x_5 y_3, \qquad b_1 = y_3 - y_5, \qquad c_1 = x_5 - x_3, \tag{2-1}$$

with the remaining expressions following by permutation of the suffices. The area of the element is denoted by A where

$$2A = b_3 c_5 - b_5 c_3 \ . \tag{2-2}$$

The theory of conforming triangular plate bending elements with cubically varying w-displacement along the sides is well documented[1,2,3]; the connection properties are illustrated in Fig.3b where the mid-side connection points are present in recognition of the correct quadratic variation of $\partial w/\partial n$ along the sides. From the very practical viewpoint of efficient computation, however, it is desirable to eliminate these mid-side connections because, as discussed in the Introduction, they are responsible for a disproportionately large increase in both the bandwidth and in the total number of rows in the global stiffness matrix. Their elimination by the simple expediency of linearizing[1,2] the normal derivative $\partial w/\partial n$ along the sides of the triangular elements is found to be unsatisfactory because the constraints which are thereby imposed lead to an unacceptably overstiff solution. Clearly, a more precise interpolation for this mid-side value of $\partial w/\partial n$ is worth investigating where, at least, a partial aim must be the exact recovery of all solutions where the displaced shape $w(x,y)$ is described in terms of the general surface cubic.

In what follows, the value of each mid-side $\partial w/\partial n$ is to be interpolated from the twelve nodal connection quantities of the two triangles which share each common side. The basic topology of this extended interpolation is denoted by nodal numbers 1 2 3 4 5 6 and is illustrated in Fig.4a where the focal element is picked out by node numbers 1 3 5. The separate components of this topology are shown in Fig.4b, while the Fig.4c provides an example of a permitted variation where the nodes 2 and 4 coalesce. The listing of a Fortran computer subroutine is given in the Appendix which, when it is provided with a table of focal element node numbers like

1	0	2	0	9	0
2	0	8	0	9	0
9	0	8	0	13	0

etc.

that are appropriate to the situation shown in Fig.1c, derives the table of node numbers

1	0	2	8	9	10
2	3	8	13	9	1
9	2	8	14	13	12

etc.

which define the basic topology of our extended interpolation. The 0 in this latter table signifies that the side 1 2 coincides with the plate boundary.

Consider the component four-point topology which is denoted by node numbers 1 2 3 5 as is illustrated in Fig.4b. No loss in generality is entailed by imposing a temporary translation and rotation of the coordinate axes xOy so that the side 1 3 now lies on the Oy axis with the Ox axis passing through the mid-side point as is shown in Fig.5a. Because of this convenient reorientation of the coordinate axes, the subsidiary formulae in equations (2-1) simplify to

$$\left.\begin{aligned} a_1 = a_3 = -x_5y_3, \quad a_5 = 0; \quad b_1 = y_3 - y_5 \quad b_3 = y_3 + y_5 \quad b_5 = -2y_3; \\ c_1 = -c_3 = x_5, \quad c_5 = 0. \end{aligned}\right\} \tag{2-3}$$

We start by fitting the ten term general surface cubic to the ten connection points which remain in triangle 1 3 5 of Fig.5b when the mid-side connection $\partial^2 w_{13}/\partial x^2$ is omitted. Thus

$$w(x,y) = \sum_{j=1,3,5} (N_j w_j + N_{jx}\partial w_j/\partial x + N_{jy}\partial w_j/\partial y) + N_{13}\partial w_{13}/\partial x \tag{2-4}$$

where, on making use of equations (2-3), the shape functions $N_1, N_{1x}, \ldots$ are given by

$$\left.\begin{aligned} N_1(x,y) &= L_1 - b_1(N_{1x} + N_{3x} + N_{5x})/2A - c_1(N_{1y} + N_{3y} + N_{5y})/2A - b_1N_{13}/2A, \\ N_{1x}(x,y) &= -c_1L_1L_5(L_3 - L_1), \\ N_{1y}(x,y) &= L_1(2b_1L_3L_5 + b_3L_1L_5 - b_5L_1L_3), \\ N_3(x,y) &= L_3 - b_3(N_{1x} + N_{3x} + N_{5x})/2A + c_1(N_{1y} + N_{3y} + N_{5y})/2A - b_3N_{13}/2A, \\ N_{3x}(x,y) &= c_1L_3L_5(L_3 - L_1), \\ N_{3y}(x,y) &= -L_3(2b_3L_1L_5 + b_1L_3L_5 - b_5L_1L_3), \\ N_5(x,y) &= L_5 - b_5(N_{1x} + N_{3x} + N_{5x})/2A - b_5N_{13}/2A, \\ N_{5x}(x,y) &= -c_1L_5^2(L_1 + L_3), \\ N_{5y}(x,y) &= L_5^2(b_1L_3 - b_3L_1), \\ N_{13}(x,y) &= 4c_1L_1L_3L_5, \end{aligned}\right\} \tag{2-5}$$

where A denotes the area of the triangle 1 3 5 and, from equations (2-2) and (2-3),

$$2A = -b_5c_3 = 2a_1 = 2a_3 = -2x_5y_3 \ . \tag{2-6}$$

At the middle of side 1 3 we note that the second differentials of these shape functions with respect to x are given by

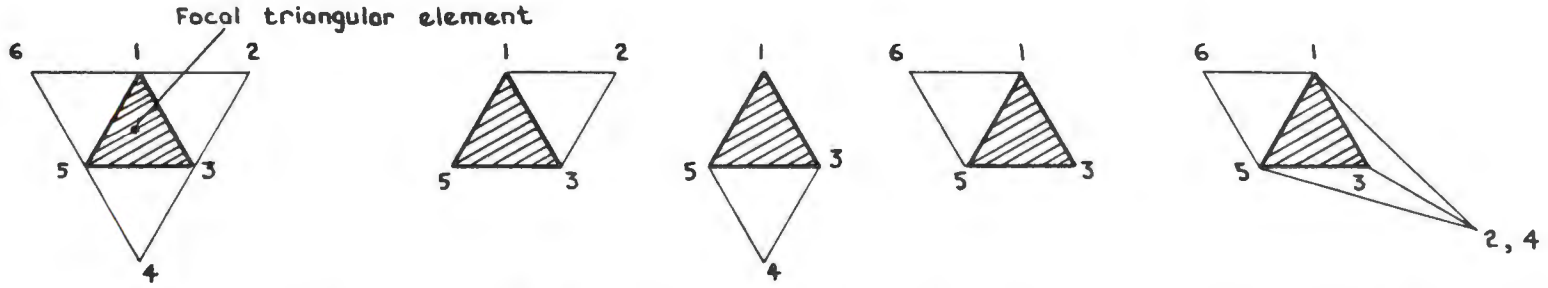

Fig. 4a Six point basic topology

Fig. 4b Component four point topologies

Fig. 4c Example of permitted variation in basic topology

Fig. 4 Topology of extended interpolation for element with cubically varying w displacement along the side

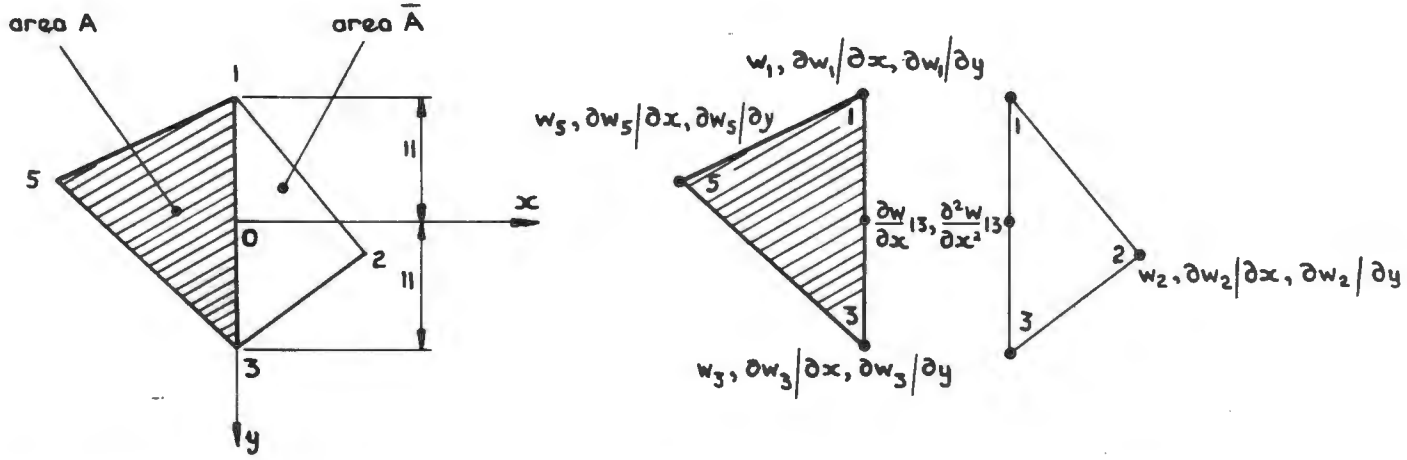

Fig. 5a Temporary change of coordinate axes

Fig. 5b Connection properties for extended interpolation procedure

Fig. 5 Coordinate axes and connection properties for extended interpolation procedure

$$
\left.\begin{aligned}
\partial^2 N_1/\partial x^2 &= -3y_3(y_3 - y_5)/A^2, & \partial^2 N_3/\partial x^2 &= -3y_3(y_3 + y_5)/A^2,\\
\partial^2 N_1/\partial x^2 &= -y_5/A, & \partial^2 N_{3x}/\partial x^2 &= y_5/A,\\
\partial^2 N_{1y}/\partial x^2 &= -y_3(3y_3 + y_5)(y_3 - y_5)/2A^2, & \partial^2 N_{3y}/\partial x^2 &= y_3(3y_3 - y_5)(y_3 + y_5)/2A^2,\\
\partial^2 N_5/\partial x^2 &= 6y_3^2/A^2, & & \\
\partial^2 N_{5x}/\partial x^2 &= 2y_3/A, & \partial^2 N_{13}/\partial x^2 &= 4y_3/A.\\
\partial^2 N_{5y}/\partial x^2 &= -2y_3^2 y_5/A^2, & &
\end{aligned}\right\} \quad (2\text{-}7)
$$

In an entirely similar way for the triangle 1 2 3 of Fig.5b the cubic $w(x,y)$ is defined by

$$
\begin{aligned}
w(x,y) = {} & \bar{N}_1 w_1 + \bar{N}_{1x}\partial w_1/\partial x + \bar{N}_{1y}\partial w_1/\partial y\\
& + N_2 w_2 + N_{2x}\partial w_2/\partial x + N_{2y}\partial w_2/\partial y\\
& + \bar{N}_3 w_3 + \bar{N}_{3x}\partial w_3/\partial x + \bar{N}_{3y}\partial w_3/\partial y + N_{31}\partial w_{31}/\partial x
\end{aligned} \quad (2\text{-}8)
$$

where the formulae for the shape functions are like those given in equation (2-5).

A satisfactorily high level of continuity is achieved across the interface 1 3 of the two triangles shown in Fig.5b by ensuring that, at the mid-side,

$$
\partial^2 w_{13}/\partial x^2 = \partial^2 w_{31}/\partial x^2 \quad (2\text{-}9)
$$

in addition to the continuities which equations (2-4) and (2-8) already provide across this interface. This equation (2-9) serves to define the interpolation formula for $\partial w_{13}/\partial x$ because, on substitution from equations (2-4) and (2-8), we obtain

$$
I_{13}\partial w_{13}/\partial x = I_{13}\partial w_{31}/\partial x = \sum_{j=1,2,3,5} (I_j w_j + I_{jx}\partial w_j/\partial x + I_{jy}\partial w_j/\partial y) \quad (2\text{-}10)
$$

where the constants $I_{13}, I_1, I_{1x}, \ldots$ are explicitly

$$
\left.\begin{aligned}
I_{13} &= 4(1/A + 1/\bar{A}),\\
I_1 &= 3\{(y_3 - y_5)/A^2 + (y_2 - y_3)/\bar{A}^2\}, & I_{1x} &= (y_5/A + y_2/\bar{A})/y_3,\\
I_{1y} &= (3y_3 + y_5)(y_3 - y_5)/2A^2 + (y_2 + 3y_3)(y_2 - y_3)/2\bar{A}^2,\\
I_2 &= 6y_3/\bar{A}^2, & I_{2x} &= -2/\bar{A}, & I_{2y} &= -2y_2 y_3/\bar{A}^2,\\
I_3 &= 3\{(y_3 + y_5)/A^2 - (y_2 + y_3)/\bar{A}^2\}, & I_{3x} &= -I_{1x},\\
I_{3y} &= -(3y_3 - y_5)(y_3 + y_5)/2A^2 - (y_2 - 3y_3)(y_2 + y_3)/2\bar{A}^2,\\
I_5 &= -6y_3/A^2, & I_{5x} &= -2/A, & I_{5y} &= 2y_3 y_5/A^2,
\end{aligned}\right\} \quad (2\text{-}11)
$$

where $\bar{A}$ is the area of the triangle 1 2 3

$$2\bar{A} = 2x_2y_3 . \qquad (2\text{-}12)$$

It can be confirmed that equation (2-10) provides the exact value for $\partial w_{13}/\partial x$ whenever $w(x,y)$ is a general surface cubic and, moreover, when the temporary reorientation of the coordinate axes is reversed, see equation (2-3), it is a simple matter then to derive the corresponding estimate for the normal derivative $\partial w_{13}/\partial n$.

The interpolation formulae for the remaining mid-side normal derivatives $\partial w_{35}/\partial n$ and $\partial w_{51}/\partial n$ of the focal triangle 1 3 5 may be written down in like manner. While shortage of space does not allow details to be given here, a matrix interpolation scheme can be arranged to eliminate all traces of $\partial w_{13}/\partial n$, $\partial w_{35}/\partial n$ and $\partial w_{51}/\partial n$ from the element stiffness matrix. Such a scheme has been set up and applied by Morley and Merrifield[3] to the conforming plate bending triangular element with cubically varying displacement w. Their element is essentially that described by Bazeley *et al*[2] and employs rational functions to supplement the ten term cubic description of the displacement $w(x,y)$ within the finite element; their bending moments are, however, calculated on a novel basis which makes use of a homogeneous equilibrium field within the element. Numerical results of calculations for the classical problems of the square plate are listed in Tables 1 and 2 where only a quarter of the plate is considered with the finite element mesh as shown in Fig.1; the plate has side length L and Poisson's ratio $\nu = 0.3$. It is to be remarked that there is little difference between the results which are secured by retaining the mid-side connection property and those obtained here with the aid of extended interpolation. What is more, the size of the global stiffness matrix now more nearly resembles that which is required for the non-conforming element of Bazeley *et al*[2] whose comparative results for the displacements are also quoted in Table 1. The results from extended interpolation are, incidentally, in good agreement with the exact values.

3. PLATE BENDING ELEMENT WITH QUADRATICALLY VARYING w-DISPLACEMENT

It is shown elsewhere[8] that if a straightforward application of the familiar theorem of minimum potential energy is made with a plate bending triangular element where the displacement $w(x,y)$ varies quadratically and where the (non-conforming) connection properties are as shown in Fig.2a, then this is exactly equivalent to a correct application of the theorem of minimum complementary energy. Furthermore, since this constant bending moment equilibrium element is used in conjunction with a complete set of coordinate/shape functions there is also an assuredness of convergence to the exact solution during progression to successively finer meshes. Encouraged by the success of our previous application of the idea of extended interpolation, it is tempting to enquire whether there is benefit to be gained here by eliminating the mid-side connection points of Fig.2a so as to provide the simplest possible connection properties for a plate bending element, i.e. those which concern merely the value of the displacement w at the three nodes of the triangle as is illustrated in Fig.2b. In the examination which is given below it is convenient, especially in view of the algebraic simplicity, to provide a complete derivation of the element pseudo-stiffness matrix. It should be noted, however, that in the equilibrium model the connection quantities,

Table 1

CENTRAL DEFLECTION OF A SQUARE PLATE USING CONFORMING PLATE BENDING TRIANGULAR ELEMENTS WITH CUBICALLY VARYING EDGE DISPLACEMENT w

	With extended inter-polation	With mid-side connection points	Non-conforming element[2]	Exact	Multiplier
UDL simply supported	0.004065	0.004064	0.00405	0.00406	q_0L^4/D
UDL clamped	0.001257	0.001258	0.00134	0.00126	q_0L^4/D
conc. load simply supported	0.01151	0.01152	0.01165	0.0116	PL^2/D
conc. load clamped	0.005488	0.005494	0.00572	0.00560	PL^2/D
global stiffness matrix					
rows	75	131	75		
semi-bandwidth	36	35	30		

Table 2

BENDING MOMENTS IN A SQUARE PLATE USING CONFORMING PLATE BENDING TRIANGULAR ELEMENTS WITH CUBICALLY VARYING EDGE DISPLACEMENT w

	Centre of side	Centre of plate		Corner reaction	Multiplier
	M_n	M_x	M_y	$\lvert 2M_{xy} \rvert$	
UDL simply supported		0.0488 0.0493* (0.0479)	0.0500 0.0502* (0.0479)	0.0688 0.0686* (0.065)	q_0L^2
UDL clamped	-0.0481 -0.0476* (-0.0513)	0.0240 0.0240* (0.0231)	0.0245 0.0243* (0.0231)		q_0L^2
conc. load simply supported				0.126 0.126* (0.122)	P
conc. load clamped	-0.1199 -0.1172* (-0.1257)				P

The first value, in each case, is obtained with the aid of extended interpolation. *The asterisked value is obtained with the retention of the mid-side connection property. (The value in parentheses is exact).

The numerical results in Tables 1 and 2 are obtained by considering a quarter of the square plate where the finite element mesh is as shown in Fig.1.

like w_1 and $\partial w_{15}/\partial n$, are really Lagrangian multipliers which serve to enforce traction continuity across the element interfaces and, consequently, their estimation by other than the strict variational process generally undermines this traction continuity as well as the bounded property of the variational principle.

The triangular finite element of arbitrary shape is shown in Fig.2 where it is now expedient to number the nodes 1 5 9. A point within the element is located by the non-dimensional area coordinates L_1, L_5 and L_9 where, cf. equation (2-1),

$$\left.\begin{aligned} L_1 &= (a_1 + b_1 x + c_1 y)/2A, \\ a_1 &= x_5 y_9 - x_9 y_5, \quad b_1 = y_5 - y_9, \quad c_1 = x_9 - x_5, \end{aligned}\right\} \tag{3-1}$$

with the remaining expressions following by permutation of the suffices. The area A of the triangular element is here

$$2A = b_5 c_9 - b_9 c_5 \ . \tag{3-2}$$

The coordinate s is taken clockwise around the boundary of the element and the length of the side joining nodes 1 and 5 is denoted by s_{15} where

$$s_{15}^2 = b_9^2 + c_9^2 \ . \tag{3-3}$$

The outward pointing normal n from this side subtends the angle γ_{15} with the Ox coordinate axis and it is easily verified that

$$\sin \gamma_{15} = -c_9/s_{15}, \quad \cos \gamma_{15} = -b_9/s_{15} \ . \tag{3-4}$$

The artifice described by Bazeley *et al*[2] is followed so that the actual displacement of the element is described by

$$w = w' + w^R \tag{3-5}$$

where w^R is the rigid body displacement

$$w^R(x,y) = w_1 L_1 + w_5 L_5 + w_9 L_9 \tag{3-6}$$

which contributes nothing to the curvatures and $w'(x,y)$ is the relative displacement of the element when it is regarded as supported at the nodes, i.e.

$$w_1' = w_5' = w_9' = 0 \ . \tag{3-7}$$

The normal slope of the displaced element surface at the mid-side 1 5 is denoted by $\partial w_{15}/\partial n$, see Fig.2a, with

$$\partial w_{15}/\partial n = (\partial w_{15}/\partial x) \cos \gamma_{15} + (\partial w_{15}/\partial y) \sin \gamma_{15} \tag{3-8}$$

where the derivatives $\partial w_{15}/\partial x$ and $\partial w_{15}/\partial y$ also refer to this mid-side point. It follows from equation (3-5), typically for this side, that

$$\partial w_{15}/\partial n = \partial w_{15}'/\partial n + \partial w_{15}^R/\partial n \ . \tag{3-9}$$

The quadratically varying relative deflection w' is now written

$$w'(x,y) = N_{15}\partial w'_{15}/\partial n + N_{59}\partial w'_{59}/\partial n + N_{91}\partial w'_{91}/\partial n \qquad (3\text{-}10)$$

with shape function

$$N_{15}(x,y) = -2AL_9(1 - L_9)/s_{15} \qquad (3\text{-}11)$$

and $N_{59}(x,y)$, $N_{91}(x,y)$ following by permutation of the suffices. The shape function $N_{15}(x,y)$ is zero at all three node points, as is required for support, while the first derivatives

$$\partial N_{15}/\partial x = b_9(2L_9 - 1)/s_{15}, \qquad \partial N_{15}/\partial y = c_9(2L_9 - 1)/s_{15} \qquad (3\text{-}12)$$

are zero at the mid-sides 5 9 and 9 1; along the side 1 5, however, they are constant with

$$\partial N_{15}/\partial n = (\partial N_{15}/\partial x)\cos\gamma_{15} + (\partial N_{15}/\partial y)\sin\gamma_{15} = 1 \qquad (3\text{-}13)$$

which follows on using equations (3-3) and (3-4).

The variation of the virtual work contribution by the element is given by

$$\delta U^e = \{\delta q'\}^{eT}[k']^e\{q'\}^e + \{\delta q'\}^{eT}\{F^{*'}\}^e + \{\delta q^R\}^{eT}\{F^{*R}\}^e \qquad (3\text{-}14)$$

where the 3 by 1 column matrices of generalised displacements are

$$\{q'\}^e = (\partial w'_{15}/\partial n \;\; \partial w'_{59}/\partial n \;\; \partial w'_{91}/\partial n)^T, \qquad \{q^R\}^e = (w_1 \;\; w_5 \;\; w_9)^T \quad . \qquad (3\text{-}15)$$

The stiffness matrix is most easily derived by way of a preliminary application of Green's theorem to the customary surface integral for the strain energy so that, for the constant thickness element,

$$\{\delta q'\}^{eT}[k']^e\{q'\}^e = -\int M_n\partial\delta w'/\partial n\, ds = -\{\delta q'\}^{eT}(s_{15}M_{n_{15}} \;\; s_{59}M_{n_{59}} \;\; s_{91}M_{n_{91}})^T \quad . \qquad \ldots\ (3\text{-}16)$$

This equation enjoys such a simple form because the Kirchhoff force is zero along each side of the element and because the relative displacement $w'(x,y)$ satisfies $\nabla^4 w' = 0$ over the whole surface of the element as well as $w' = 0$ at the nodes. Typically, $M_{n_{15}}$ is the normal bending moment which is acting on the side 1 5 and is calculated by substituting equations (3-10) into the usual moment-displacement relations together with

$$M_{n_{15}} = M_x\cos^2\gamma_{15} + M_y\sin^2\gamma_{15} - 2M_{xy}\sin\gamma_{15}\cos\gamma_{15}. \qquad (3\text{-}17)$$

It follows for the particular case of the isotropic plate that the first three constituents of the 3 by 3 relative stiffness matrix $[k']^e$ are given by

$$\left.\begin{aligned} k'_{11} &= Ds_{15}^2/A, \\ k'_{12} &= k'_{21} = D\{b_1^2(b_9^2+\nu c_9^2) + c_1^2(c_9^2+\nu b_9^2) + 2(1-\nu)b_1b_9c_1c_9\}/As_{59}s_{15}, \\ k'_{13} &= k'_{31} = D\{b_5^2(b_9^2+\nu c_9^2) + c_5^2(c_9^2+\nu b_9^2) + 2(1-\nu)b_5b_9c_5c_9\}/As_{91}s_{15}, \end{aligned}\right\} \qquad (3\text{-}18)$$

where substitutions are made from equations (3-4) and the flexural rigidity is defined in the usual way by $D = Eh^3/12(1 - \nu^2)$ with E as the Young's modulus, h the plate thickness and ν the Poisson's ratio. The element load matrices $\{F^{*\prime}\}^e$ and $\{F^{*R}\}^e$ are concerned only with the contributions which arise from applied bending moments at the plate boundary; the virtual work from any applied normal force is more easily incorporated at global level. As an illustrative example we consider the situation where only one side, e.g. 1 5, of the element coincides with the plate boundary where the mid-side normal bending moment is prescribed as

$$M_{n_{15}} = M^*_{n_{15}} \quad . \tag{3-19}$$

The element load matrices are then easily found to be

$$\left.\begin{aligned} \{F^{*\prime}\}^e &= s_{15} M^*_{n_{15}} (1 \;\; 0 \;\; 0)^T, \\ \{F^{*R}\}^e &= -(M^*_{n_{15}}/2A)(b_1 b_9 + c_1 c_9 \;\; b_5 b_9 + c_5 c_9 \;\; s_{15})^T. \end{aligned}\right\} \tag{3-20}$$

The normal derivatives of the relative displacement, i.e. the $\partial w'/\partial n$, at the mid-side points of the triangular element are now to be estimated in terms of the actual deflection w at the nodes of nearby elements. The basic topology for this extended interpolation is slightly more complicated than that which was required in section 2; it is described by twelve node numbers 1 2 3 4 5 6 7 8 9 10 11 12 as is shown in Fig.6 where the focal element is picked out by the node numbers 1 5 9. Variations on the topology are permitted provided that at least four triangular elements share each node which does not lie on the plate boundary; the topology is arbitrary for nodes actually on the boundary. The extended interpolation is to be arranged in such a way that exact values are derived for the mid-side normal derivatives $\partial w/\partial n$ in all cases where the true global displaced shape $w(x,y)$ is describable in terms of the general surface quadratic; moreover, the value of $\partial w/\partial n$ is required to be uniquely determined in any progression to an adjacent focal element. The Fortran computer subroutine, which is listed in the Appendix, serves also to define the basic topology for this new extended interpolation; when it is provided with a table of focal element node numbers like

```
1  0  0  0  2  0  0  0  9  0  0  0
2  0  0  0  8  0  0  0  9  0  0  0
9  0  0  0  8  0  0  0 13  0  0  0
etc.
```

which are again appropriate to the situation shown in Fig.1c, it calculates the required table of node numbers

```
1  0  0  0  2  3  8 13  9 12 10  0
2  0  3  7  8 14 13 12  9 10  1  0
9  1  2  3  8  7 14 17 13 18 12 10
etc..
```

Let us begin by considering the component six-point topology 1 3 5 7 9 11 which completely surrounds the focal element 1 5 9 as is shown in Fig.6b. Equation (3-10) immediately provides the relative deflections w'_3, w'_7 and w'_{11} where

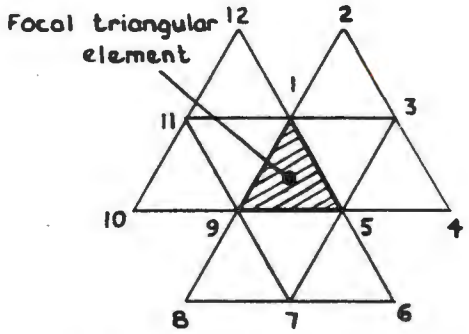

Fig. 6a Twelve point basic topology

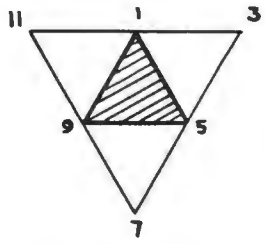

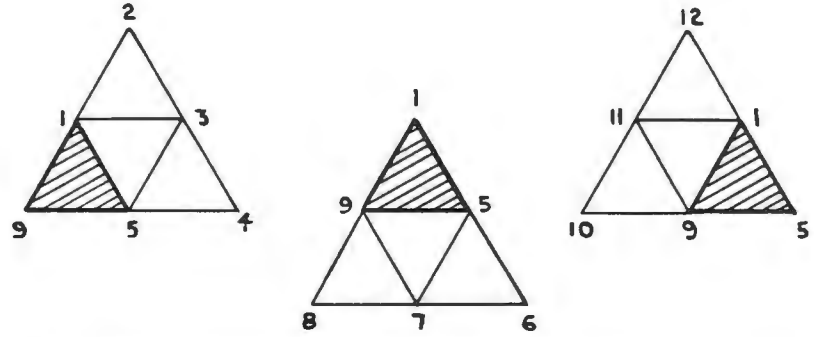

Fig. 6b Component six point topologies

Fig. 6 Topology of extended interpolation for element with quadratically varying displacements

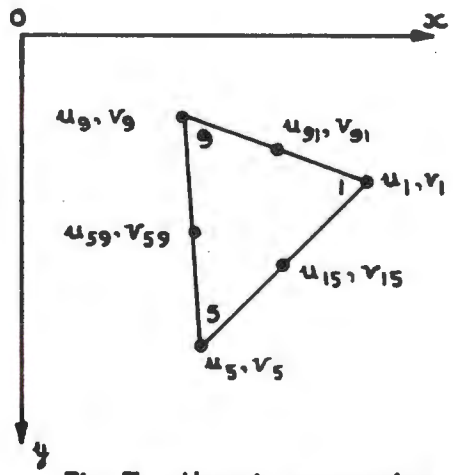

Fig. 7a Usual connection properties

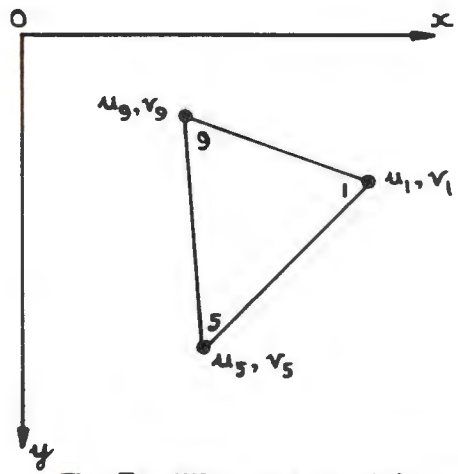

Fig. 7b With extended interpolation

Fig. 7 Connection properties of plane stress element with quadratically varying displacements

$$\begin{Bmatrix} w'_3 \\ w'_7 \\ w'_{11} \end{Bmatrix} = \begin{bmatrix} N_{15}(x_3,y_3) & N_{59}(x_3,y_3) & N_{91}(x_3,y_3) \\ N_{15}(x_7,y_7) & N_{59}(x_7,y_7) & N_{91}(x_7,y_7) \\ N_{15}(x_{11},y_{11}) & N_{59}(x_{11},y_{11}) & N_{91}(x_{11},y_{11}) \end{bmatrix} \begin{Bmatrix} \partial w'_{15}/\partial n \\ \partial w'_{59}/\partial n \\ \partial w'_{91}/\partial n \end{Bmatrix} . \quad (3\text{-}21)$$

The square matrix in this equation is required to be non-singular and it is in this context that the above mentioned topological restriction is important. There are also exceptional arrangements of mesh geometry which must be avoided, like a colinearity of the four nodes numbered 1 3 7 9 in the first of the topological descriptions of Fig.6b. Fortunately, however, the simple requirement that no finite element contains an obtuse angle is sufficient, although by no means necessary, to provide an essentially non-singular matrix. Such restriction on the triangular element shape is of minor practical importance, it is rather one more exhortation towards sound finite element practice. A simple inversion of the 3 by 3 matrix of equation (3-21) now gives

$$\begin{Bmatrix} \partial w'_{15}/\partial n \\ \partial w'_{59}/\partial n \\ \partial w'_{91}/\partial n \end{Bmatrix} = \begin{bmatrix} N_{15}(x_3,y_3) & N_{59}(x_3,y_3) & N_{91}(x_3,y_3) \\ N_{15}(x_7\ y_7) & N_{59}(x_7,y_7) & N_{91}(x_7,y_7) \\ N_{15}(x_{11},y_{11}) & N_{59}(x_{11},y_{11}) & N_{91}(x_{11},y_{11}) \end{bmatrix}^{-1} \begin{Bmatrix} w'_3 \\ w'_7 \\ w'_{11} \end{Bmatrix} . \quad (3\text{-}22)$$

While this equation (3-22) provides a reasonable estimate for the value of $\partial w'_{15}/\partial n$, for example, it is noted from the component six-point topology 1 2 3 4 5 9 of Fig.6b that we may derive also

$$\begin{Bmatrix} \partial w'_{15}/\partial n \\ \partial w'_{59}/\partial n \\ \partial w'_{91}/\partial n \end{Bmatrix} = \begin{bmatrix} N_{15}(x_2,y_2) & N_{59}(x_2,y_2) & N_{91}(x_2,y_2) \\ N_{15}(x_3,y_3) & N_{59}(x_3,y_3) & N_{91}(x_3,y_3) \\ N_{15}(x_4,y_4) & N_{59}(x_4,y_4) & N_{91}(x_4,y_4) \end{bmatrix}^{-1} \begin{Bmatrix} w'_2 \\ w'_3 \\ w'_4 \end{Bmatrix} \quad (3\text{-}23)$$

which gives an equally reasonable, albeit generally different, estimate for $\partial w_{15}/\partial n$. Several courses of action are now available but our preference is to take the arithmetic mean of the two estimates with the assurance that the value is then always uniquely estimated, irrespectively of whether the focal triangle is 1 5 9 or 1 3 5. The equations (3-5) and (3-6) show that the relative displacements w'_3, w'_7, w'_{11} of equation (3-22), for example, may subsequently be transformed into actual displacements w by the matrix transformation

$$\begin{Bmatrix} w'_3 \\ w'_7 \\ w'_{11} \end{Bmatrix} = \begin{bmatrix} -L_1(x_3,y_3) & 1 & -L_5(x_3,y_3) & 0 & -L_9(x_3,y_3) & 0 \\ -L_1(x_7,y_7) & 0 & -L_5(x_7,y_7) & 1 & -L_9(x_7,y_7) & 0 \\ -L_1(x_{11},y_{11}) & 0 & -L_5(x_{11},y_{11}) & 0 & -L_9(x_{11},y_{11}) & 1 \end{bmatrix} \begin{Bmatrix} w_1 \\ w_3 \\ w_5 \\ w_7 \\ w_9 \\ w_{11} \end{Bmatrix} . \quad (3\text{-}24)$$

It remains to deal with cases such as where the side 1 5 is coincident with the plate boundary so that the node number 3, see Fig.6, does not even exist. The simplest case occurs when the mid-side kinematic boundary condition is prescribed

$$\partial w_{15}/\partial n = \partial w^{*}_{15}/\partial n \qquad (3\text{-}25)$$

because, from equations (3-5), (3-6) and (3-9) the normal derivative $\partial w'_{15}/\partial n$ of the corresponding relative displacement is then given directly in terms of nodal displacements by

$$\partial w'_{15}/\partial n = -\{(b_1 w_1 + b_5 w_5 + b_9 w_9)\cos\gamma_{15} + (c_1 w_1 + c_5 w_5 + c_9 w_9)\sin\gamma_{15}\}/2A + \partial w^{*}_{15}/\partial n \ . \qquad (3\text{-}26)$$

One way of dealing with the mid-side traction boundary conditions, like the normal bending moment which is prescribed by equation (3-19), is to substitute from the matrix equations (3-16) and (3-20) to obtain, in this instance,

$$\{k'_{11}\partial w'_{15}/\partial n + k'_{12}\partial w'_{59}/\partial n + k'_{13}\partial w'_{91}/\partial n + F^{*'}_1\}\ \delta\partial w'_{15}/\partial n = 0 \ . \qquad (3\text{-}27)$$

Equation (3-21) can then be replaced with

$$\begin{Bmatrix} 0 \\ w'_7 \\ w'_{11} \end{Bmatrix} = \begin{bmatrix} k'_{11} & k'_{12} & k'_{13} \\ N_{15}(x_7,y_7) & N_{59}(x_7,y_7) & N_{91}(x_7,y_7) \\ N_{15}(x_{11},y_{11}) & N_{59}(x_{11},y_{11}) & N_{91}(x_{11},y_{11}) \end{bmatrix} \begin{Bmatrix} \partial w'_{15}/\partial n \\ \partial w'_{59}/\partial n \\ \partial w'_{91}/\partial n \end{Bmatrix} + \begin{Bmatrix} F^{*'}_1 \\ 0 \\ 0 \end{Bmatrix} \qquad \ldots. \ (3\text{-}28)$$

where the square matrix is inverted to provide a relationship similar to that of equation (3-22) but with the addition of a column vector of constants.

In what follows, it is convenient to suppose that all the above is summarised into a matrix interpolation scheme for the focal triangular element 1 5 9 in such a way that

$$\{q'\}^e = [\,I\,]\{q_I\}^e + \{i\} \qquad (3\text{-}29)$$

where the 3 by 1 column vector of mid-side connection quantities $\{q'\}^e$ is as given by equation (3-15), $[\,I\,]$ is a 3 by 12 rectangular matrix of constants, the column vector of nodal connection quantities $\{q_I\}^e$ is defined by

$$\{q_I\}^e = (w_1\ w_2\ w_3\ \ldots\ w_{12})^T, \qquad (3\text{-}30)$$

and $\{i\}$ is a 3 by 1 column vector of constants. Thus, when equation (3-29) is substituted into equation (3-14) the variation δU^e of the virtual work contribution by the element becomes

$$\delta U^e = \{\delta q_I\}^{eT}[\,I\,]^T[k']^e[\,I\,]\{q_I\}^e + \{\delta q_I\}^{eT}[\,I\,]^T[k']^e\{i\} + \{\delta q_I\}^{eT}[\,I\,]^T\{F^{*'}\}^e + \{\delta q^R\}^{eT}\{F^{*R}\}^e \qquad (3\text{-}31)$$

which is now in terms only of actual nodal displacements.

Although, as already noted, the interpolation of the mid-side value of the normal derivative $\partial w/\partial n$ destroys the strict equilibrium nature of this plate bending element, the Tables 3 and 4 show that it frequently provides agreeable improvements in the accuracy of the numerical results

Table 3

CENTRAL DEFLECTION OF A SQUARE PLATE USING TRIANGULAR ELEMENTS WITH QUADRATICALLY VARYING w-DISPLACEMENT

	With extended interpolation	With mid-side connection points	Non-conforming element[1]	Exact	Multiplier
UDL simply supported	0.00411 {0.00414}	0.00432 {0.00412}	0.00405	0.00406	q_0L^4/D
UDL clamped	0.00154 {0.00134}	0.00170 {0.00138}	0.00134	0.00126	q_0L^4/D
conc. load simply supported	0.01315 {0.01207}	0.01351 {0.01219}	0.01165	0.0116	PL^2/D
conc. load clamped	0.00727 {0.00611}	0.00776 {0.00628}	0.00572	0.00560	PL^2/D
global stiffness matrix					
rows	25 {81}	81 {289}	75		
semi-bandwidth	20 {36}	21 {37}	30		

{The values in curly brackets refer to a finer elemental mesh where the side lengths are half those shown in Fig.1.}

Table 4

BENDING MOMENTS IN A SQUARE PLATE USING TRIANGULAR ELEMENTS WITH QUADRATICALLY VARYING w-DISPLACEMENT

	Centre of side	Centre of plate		Corner reaction	Multiplier
	M_n	M_x	M_y	$\lvert 2M_{xy} \rvert$	
UDL simply supported		0.0465 0.0471* (0.0479)	0.0436 0.0447* (0.0479)	0.057 0.065* (0.065)	q_0L^2
UDL clamped	-0.0475 -0.0443* (-0.0513)	0.0209 0.0206* (0.0231)	0.0240 0.0235* (0.0231)		q_0L^2
conc. load clamped	-0.1164 -0.1065* (-0.1257)				P

The first value, in each case, is obtained with the aid of extended interpolation. *The asterisked value is obtained with the retention of mid-side connection property. (The value in parentheses is exact.)

Except where stated, the numerical results in Tables 3 and 4 are obtained by considering a quarter of the square plate where the finite element mesh is as shown in Fig.1.

as compared with the equilibrium situation where the mid-side connection points are retained throughout the analysis. The numerical results in these Tables again refer to the classical problems of the square plate where only a quarter portion is considered, firstly with the finite element mesh as is shown in Fig.1 and secondly with a finer mesh where the side lengths are halved; again, the plate has side length L and Poisson's ratio $\nu = 0.3$. Attention is drawn to the fact that the size of the banded global stiffness matrix is now only some thirty per cent of that which is required for retention of the mid-side connection points.

4. PLANE STRESS ELEMENT WITH QUADRATICALLY VARYING DISPLACEMENTS

For our final application of the idea of extended interpolation we turn to the problem of plane stress where the displacement components u and v are assumed to vary quadratically within the triangular finite element. The usual connection properties for this element are illustrated in Fig.7a where the nodes are numbered 1 5 9. Our aim is to eliminate the mid-side connection points with the aid of extended interpolation so as to provide the preferable situation which is shown in Fig.7b where the connection properties coincide with those of the simplest of all plane stress elements in which the displacement components u and v are linearly varying; it is, however, the intention to retain much of the superior accuracy which is associated with the more complicated element. Again, it is convenient to provide a complete rederivation of the element stiffness matrix.

The quadratically varying displacement components u and v may be expressed quite generally in the form

$$\left.\begin{aligned} u(x,y) &= N_1 u_1 + N_5 u_5 + N_9 u_9 + u'(x,y), \\ v(x,y) &= N_1 v_1 + N_5 v_5 + N_9 v_9 + v'(x,y), \end{aligned}\right\} \tag{4-1}$$

where u' and v' are relative displacements defined by

$$\left.\begin{aligned} u'(x,y) &= N_{15} u_{15} + N_{59} u_{59} + N_{91} u_{91}, \\ v'(x,y) &= N_{15} v_{15} + N_{59} v_{59} + N_{91} v_{91}, \end{aligned}\right\} \tag{4-2}$$

and N_1, N_{15} are shape functions given by

$$N_1(x,y) = L_1(2L_1 - 1), \qquad N_{15}(x,y) = 4L_1 L_5 , \tag{4-3}$$

with the remaining shape functions following by permutation of the suffices. From equations (4-2) and (4-3) it is noted that the relative displacements enjoy the following properties

$$\left.\begin{aligned} &u'_1 = u'_5 = u'_9 = v'_1 = v'_5 = v'_9 = 0 , \\ &u'_{15} = u_{15}, \quad u'_{59} = u_{59}, \quad u'_{91} = u_{91} . \end{aligned}\right\} \tag{4-4}$$

The generalised strains are defined by

$$\{\varepsilon\} = \begin{Bmatrix} \partial u/\partial x \\ \partial v/\partial y \\ \partial u/\partial y + \partial v/\partial x \end{Bmatrix} = [B \quad B'] \begin{Bmatrix} q \\ q' \end{Bmatrix}^e \tag{4-5}$$

where

$$\{q\}^e = (u_1\ u_5\ u_9\ v_1\ v_5\ v_9)^T, \quad \{q'\}^e = (u_{15}\ u_{59}\ u_{91}\ v_{15}\ v_{59}\ v_{91})^T, \tag{4-6}$$

and the 3 by 6 matrices [B] and [B'] are derived by taking partial derivatives of equations (4-1) and (4-2) so that

$$[B] = \begin{bmatrix} \partial N_1/\partial x & \partial N_5/\partial x & \partial N_9/\partial x & 0 & 0 & 0 \\ 0 & 0 & 0 & \partial N_1/\partial y & \partial N_5/\partial y & \partial N_9/\partial y \\ \partial N_1/\partial y & \partial N_5/\partial y & \partial N_9/\partial y & \partial N_1/\partial x & \partial N_5/\partial x & \partial N_9/\partial x \end{bmatrix} \tag{4-7}$$

and

$$[B'] = \begin{bmatrix} \partial N_{15}/\partial x & \partial N_{59}/\partial x & \partial N_{91}/\partial x & 0 & 0 & 0 \\ 0 & 0 & 0 & \partial N_{15}/\partial y & \partial N_{59}/\partial y & \partial N_{91}/\partial y \\ \partial N_{15}/\partial y & \partial N_{59}/\partial y & \partial N_{91}/\partial y & \partial N_{15}/\partial x & \partial N_{59}/\partial x & \partial N_{91}/\partial x \end{bmatrix} \tag{4-8}$$

with, typically,

$$\left.\begin{aligned} \partial N_1/\partial x &= b_1(4L_1 - 1)/2A, & \partial N_1/\partial y &= c_1(4L_1 - 1)/2A, \\ \partial N_{15}/\partial x &= 4(b_1L_5 + b_5L_1)/2A, & \partial N_{15}/\partial y &= 4(c_1L_5 + c_5L_1)/2A. \end{aligned}\right\} \tag{4-9}$$

The variation δU^e of the virtual work contribution by the element is given by

$$\delta U^e = \begin{Bmatrix} \delta q \\ \delta q' \end{Bmatrix}^{eT} \begin{bmatrix} k & k' \\ k'^T & k'' \end{bmatrix}^e \begin{Bmatrix} q \\ q' \end{Bmatrix}^e + \begin{Bmatrix} \delta q \\ \delta q' \end{Bmatrix}^{eT} \begin{Bmatrix} F^* \\ F^{*\prime} \end{Bmatrix}^e \tag{4-10}$$

where the 12 by 12 element stiffness matrix is derived from

$$\begin{bmatrix} k & k' \\ k'^T & k'' \end{bmatrix}^e = \iint_A \begin{bmatrix} [B]^T[D][B] & [B]^T[D][B'] \\ \text{sym} & [B']^T[D][B'] \end{bmatrix} dA \tag{4-11}$$

The 3 by 3 elasticity matrix [D], taking as example an isotropic plate of constant thickness h, is given by

$$[D] = \frac{Eh}{1 - \nu^2} \begin{bmatrix} 1 & \nu & 0 \\ \nu & 1 & 0 \\ 0 & 0 & (1 - \nu)/2 \end{bmatrix} \tag{4-12}$$

and, in evaluating the area integrals of equation (4-11), it is helpful to note the standard forms

$$\iint_A L_1 dA = 2\iint_A L_1^2 dA = 4\iint_A L_1 L_5 dA = A/3. \qquad (4\text{-}13)$$

The 3 by 1 element load matrices $\{F^*\}^e$ and $\{F^{*'}\}^e$ are calculated in the usual manner. By way of illustration, if it is assumed that only the side 1 5 coincides with the plate boundary where the following tractions are prescribed

$$\sigma_{n_1} = \sigma^*_{n_1}, \quad \tau_{ns_1} = \tau^*_{ns_1}, \quad \sigma_{n_5} = \sigma^*_{n_5}, \quad \tau_{ns_5} = \tau^*_{ns_5}, \qquad (4\text{-}14)$$

then the load matrix $\{F^{*'}\}^e$, which is of special interest in the present context of extended interpolation is, in the absence of surface forces,

$$\{F^{*'}\}^e = -(s_{15}/3)\begin{Bmatrix} (\sigma^*_{n_1} + \sigma^*_{n_5}) \cos\gamma_{15} - (\tau^*_{ns_1} + \tau^*_{ns_5}) \sin\gamma_{15} \\ 0 \\ 0 \\ (\sigma^*_{n_1} + \sigma^*_{n_5}) \sin\gamma_{15} + (\tau^*_{ns_1} + \tau^*_{ns_5}) \cos\gamma_{15} \\ 0 \\ 0 \end{Bmatrix} . \qquad (4\text{-}15)$$

The mid-side displacement values like u_{15} and v_{15}, which constitute the column vector $\{q'\}^e$ of equation (4-6), are now to be estimated in terms of the displacements at the nodes of nearby elements. The general details of the mesh topology for the purpose of this plane stress extended interpolation are the same as are described in section 3, see Fig.6. The interpolation is again to be arranged in such a way that exact values are recovered for the mid-side displacements whenever the true displaced state $u(x,y)$, $v(x,y)$ is describable in terms of the general surface quadratic. It is of especial importance, also, that these mid-side displacements are uniquely determined so as to preserve the bounded property which belongs to correct applications of the theorem of minimum potential energy.

The six point component topology which is denoted by node numbers 1 3 5 7 9 11 is shown in Fig.6b to encircle the focal element 1 5 9 and the equations (4-2) for the relative displacements provide

$$\begin{Bmatrix} u'_3 \\ u'_7 \\ u'_{11} \end{Bmatrix} = \begin{bmatrix} N_{15}(x_3,y_3) & N_{59}(x_3,y_3) & N_{91}(x_3,y_3) \\ N_{15}(x_7,y_7) & N_{59}(x_7,y_7) & N_{91}(x_7,y_7) \\ N_{15},(x_{11},y_{11}) & N_{59}(x_{11},y_{11}) & N_{91}(x_{11},y_{11}) \end{bmatrix} \begin{Bmatrix} u_{15} \\ u_{59} \\ u_{91} \end{Bmatrix} . \qquad (4\text{-}16)$$

The sufficient conditions for the square matrix in this equation to be non-singular are identical with those already described for equation (3-21). The 3 by 3 matrix of equation (4-16) may then be inverted to give

$$\begin{Bmatrix} u_{15} \\ u_{59} \\ u_{91} \end{Bmatrix} = \begin{bmatrix} N_{15}(x_3,y_3) & N_{59}(x_3,y_3) & N_{91}(x_3,y_3) \\ N_{15}(x_7,y_7) & N_{59}(x_7,y_7) & N_{91}(x_7,y_7) \\ N_{15}(x_{11},y_{11}) & N_{59}(x_{11},y_{11}) & N_{91}(x_{11},y_{11}) \end{bmatrix}^{-1} \begin{Bmatrix} u'_3 \\ u'_7 \\ u'_{11} \end{Bmatrix} \qquad (4\text{-}17)$$

While equation (4-17) provides a reasonable estimate for the value of the mid-side u_{15}, for example, the six point topology 1 2 3 4 5 9 of Fig.3b provides

$$\begin{Bmatrix} u_{15} \\ u_{59} \\ u_{91} \end{Bmatrix} = \begin{bmatrix} N_{15}(x_2,y_2) & N_{59}(x_2,y_2) & N_{91}(x_2,y_2) \\ N_{15}(x_3,y_3) & N_{59}(x_3,y_3) & N_{91}(x_3,y_3) \\ N_{15}(x_4,y_4) & N_{59}(x_4,y_4) & N_{91}(x_4,y_4) \end{bmatrix}^{-1} \begin{Bmatrix} u'_2 \\ u'_3 \\ u'_4 \end{Bmatrix} \qquad (4\text{-}18)$$

which is an equally reasonable estimate. As in section 2, there are several alternatives which are now available but, again, our preference is to take the arithmetic mean of these two estimates for u_{15} noting that this ensures a uniquely determined value irrespectively of whether the focal triangle is 1 5 9 or 1 3 5. Next, the equations (4-1) show that relative displacements like u'_3, u'_7, u'_{11} of equation (4-17) are readily expressed in terms of actual displacements by means of the matrix transformation

$$\begin{Bmatrix} u'_3 \\ u'_7 \\ u'_{11} \end{Bmatrix} = \begin{bmatrix} -N_1(x_3,y_3) & 1 & -N_5(x_3,y_3) & 0 & -N_9(x_3,y_3) & 0 \\ -N_1(x_7,y_7) & 0 & -N_5(x_7,y_7) & 1 & -N_9(x_7,y_7) & 0 \\ -N_1(x_{11},y_{11}) & 0 & -N_5(x_{11},y_{11}) & 0 & -N_9(x_{11},y_{11}) & 1 \end{bmatrix} \begin{Bmatrix} u_1 \\ u_3 \\ u_5 \\ u_7 \\ u_9 \\ u_{11} \end{Bmatrix} . \qquad (4\text{-}19)$$

The mid-side displacement components v are estimated in a similar way to that just described.

It remains to deal with the situations which arise when a side like 1 5 coincides with the plate boundary so that the node number 3 in the topology of Fig.6 does not exist. The simplest case occurs when kinematic boundary conditions are prescribed along this side for then

$$-u_{15} \sin \gamma_{15} + v_{15} \cos \gamma_{15} = u^*_{s_{15}} \qquad (4\text{-}20)$$

and/or

$$u_{15} \cos \gamma_{15} + v_{15} \sin \gamma_{15} = u^*_{n_{15}} \qquad (4\text{-}21)$$

where $u^*_{s_{15}}$ and $u^*_{n_{15}}$ are respectively the prescribed displacement components tangential and normal to the plate boundary at the mid-side point. When tractions are prescribed, it is necessary to select from equation (4-11) for the 12 by 12 element stiffness matrix the rows numbered 7 and/or 10 which, together with the rows numbered 1 and/or 4 of the element load matrix listed in equation (4-15), provide the sole global contributions to the variations δu_{15} and/or δv_{15}. Thus

$$k'_{11}u_1 + k'_{12}u_5 + k'_{13}u_9 + k'_{14}v_1 + k'_{15}v_5 + k'_{16}v_9$$
$$+ k''_{11}u_{15} + k''_{12}u_{59} + k''_{13}u_{91} + k''_{14}v_{15} + k''_{15}v_{59} + k''_{16}v_{91} = -F^{*'}_1 \quad \ldots\ (4\text{-}22)$$

and/or

$$k'_{14}u_1 + k'_{24}u_5 + k'_{34}u_9 + k'_{44}v_1 + k'_{54}v_5 + k'_{64}v_9$$
$$+ k''_{41}u_{15} + k''_{42}u_{59} + k''_{43}u_{91} + k''_{44}v_{15} + k''_{45}v_{59} + k''_{46}v_{91} = -F^{*'}_4 \ . \quad \ldots\ (4\text{-}23)$$

The requisite equations from (4-20) to (4-23) then provide enough conditions to allow both u_{15} and v_{15} to be expressed in terms of the prescribed quantities and/or the displacement components at nodes 1 5 7 9 11 together with the displacement components at mid-sides 5 9 and 9 1. Attention is drawn to the fact, however, that care needs to be exercised in dealing with these boundary situations in plane stress in order to avoid the occurrence of singular conditions. For complete reassurance it is recommended that no attempt is made to seek extended interpolation contributions from the first two of the component six point topologies in Fig.6b so that, in the present typical case, unmoderated estimates for u_{59}, u_{91} and v_{59}, v_{91} are accepted from the two remaining component topologies. The overall mesh topology can, in consequence, be no longer arbitrary for nodes actually on the boundary, indeed the recommendation requires that <u>each boundary node is at the conjunction of at least three triangular finite elements</u>.

In that which follows, it is convenient to assume that the above is summarised by a matrix interpolation scheme for the focal triangular element 1 5 9 in such a way that

$$\{q'\}^e = [I]\{q_I\}^e + \{i\} \qquad (4\text{-}24)$$

where the column vector $\{q'\}^e$ is as described by equation (4-6), $[I]$ is a 6 by 24 matrix of constants with

$$\{q_I\}^e = (u_1\ u_2\ u_3 \cdots u_{12}\ v_1\ v_2\ v_3 \cdots v_{12})^T \qquad (4\text{-}25)$$

and $\{i\}$ is a 6 by 1 column vector of constants. It is worth noting that when no nodes are missing from the twelve point basic topology of Fig.6, such as in the case of focal triangles which do not touch the plate boundary, when the 6 by 24 matrix $[I]$ may be more conveniently written as

$$[I] = \begin{bmatrix} I' & 0 \\ 0 & I \end{bmatrix} \qquad (4\text{-}26)$$

where the rectangular matrix $[I']$ is a 3 by 12 matrix of constants. By expanding the matrices of equation (4-10) we obtain the following form for the variation δU^e of the strain energy

$$\delta U^e = \{\delta q\}^{eT}[k]^e\{q\}^e + \{\delta q'\}^{eT}[k']^{eT}\{q\} + \{\delta q\}^{eT}[k']^e\{q'\} + \{\delta q'\}^{eT}[k'']^e\{q'\} + \{\delta q\}^{eT}\{F^*\}^e + \{\delta q'\}^{eT}\{F^{*'}\}^e \quad (4\text{-}27)$$

where it is now a simple matter to substitute for $\{q'\}^e$ from equation (4-24) and for $\{\delta q'\}^{eT}$ from

$$\{\delta q'\}^{eT} = \{\delta q_I\}^{eT}[I]^T \quad (4\text{-}28)$$

in order to derive the preferred form for the variation.

The numerical example concerns a square plate of side length L which is under uniform tension of σ_n^* per unit run applied parallel to the Ox axis and is weakened by a central circular hole of diameter L/2. The Poisson's ratio is taken as $\nu = 0.3$. A relatively coarse finite element mesh, see Fig.8, is employed to generate the numerical values as listed in Table 5 which contains also comparisons from other methods of solution. This problem provides a particularly severe test of any numerical technique because of the severity of the stress gradients which occur in the vicinity of the hole and also across the minimum section where there is a substantial compressive stress at the external boundary. Indeed, a comparison between the results from the continuous function solution for the infinitely long strip due to Howland[12] with that for the square plate due to Hengst[13] is illuminating in this context. Table 5 shows that whereas our finite element results for quadratically varying u,v displacements with extended interpolation provide an approximation to the more accurate finite element solution where the mid-side connection quantities are retained, it is clear that the finite element results for linearly varying u,v displacements are virtually worthless for this relatively coarse mesh. The size of the banded global stiffness matrix is seen to be less than 25 per cent of that which is required when the mid-side connections are retained; the optimal semi-bandwidths which are quoted in Table 5 are calculated by a method developed by Morley and Merrifield[14].

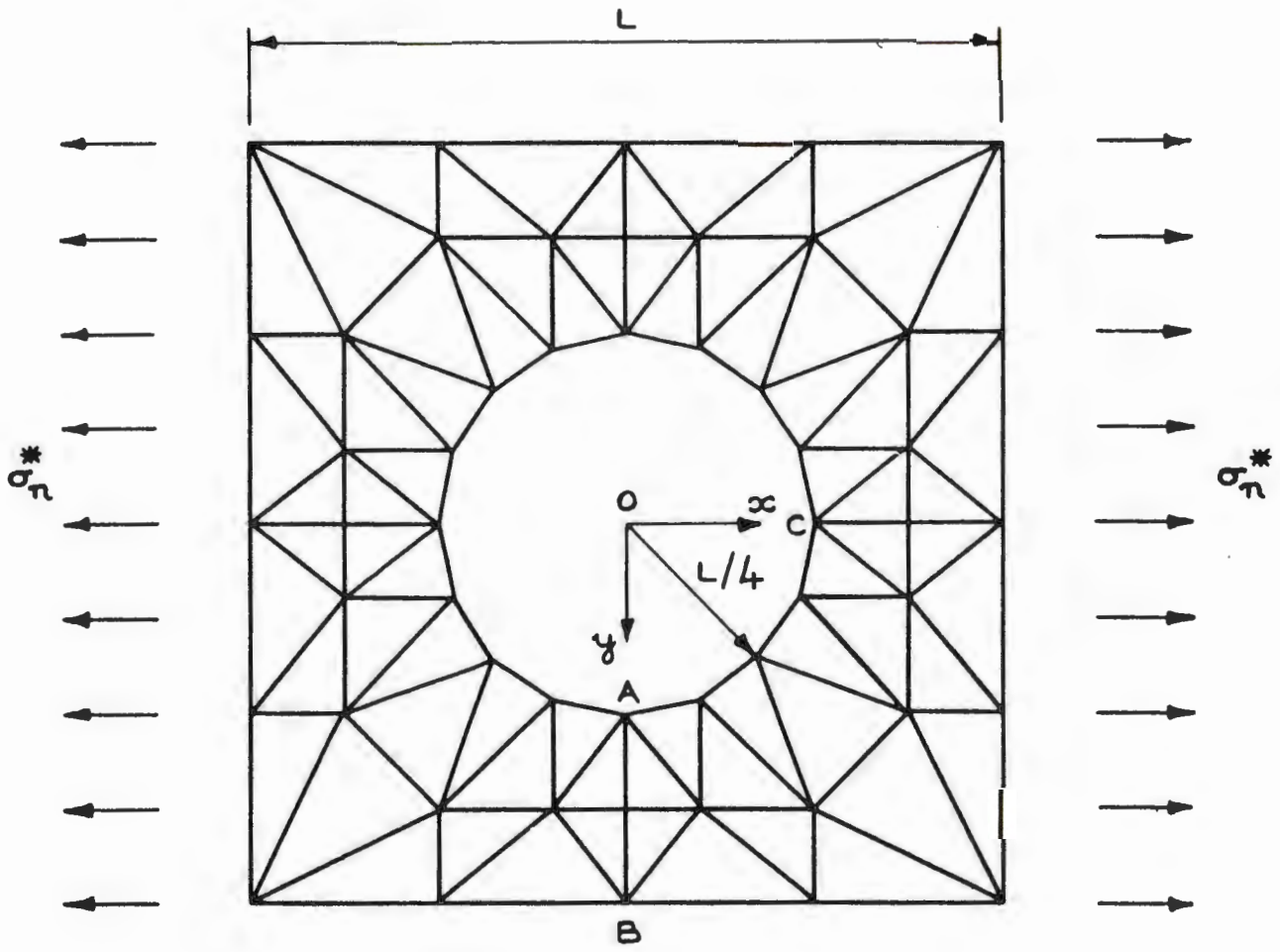

Fig. 8 Square plate under uniform tension with central circular hole

Table 5

STRESSES AND DISPLACEMENTS IN A SQUARE PLATE, UNDER UNIFORM TENSION, WITH CENTRAL CIRCULAR HOLE

	FINITE ELEMENT SOLUTIONS			CONTINUOUS FUNCTION SOLUTIONS		
	Quadratic u,v with extended interpolation	Quadratic u,v with mid-side connection points	Linear u,v	Infinite strip (Howland[12])	Square plate (Hengst[13])	Multiplier
σ_{s_A}	5.36	6.23	3.94	4.32	6.33	σ_n^*
σ_{s_B}	-0.42	-0.70	0.64	0.73		σ_n^*
σ_{s_C}	-2.81	-3.70	-1.41	-1.58	-4.11	σ_n^*
v_A	-0.884	-1.095	-0.674			$\sigma_n^* L/E$
u_C	1.525	1.734	1.233			$\sigma_n^* L/E$
global stiffness matrix						
rows	104	352	104			
optimal semi-bandwidth	40	48	16			

The displacements are appropriate to the condition that the centre of the hole does not translate or rotate.

Appendix A

FORTRAN SUBROUTINE FOR THE EXTENDED INTERPOLATION TOPOLOGY

A listing is now presented of a Fortran computer subroutine which, when it is given the basic information to define the focal-triangular elements, goes on to provide the topological description in the integer double array ELNO(NEL,JTYPE) which enables the various processes of extended interpolation to be readily performed. The notation is here

NEL = number of triangular finite elements in the plate
JTYPE = 6 or 12 depending upon the type of extended interpolation.

Thus, in the case of section 2 where a six-point extended interpolation is required for the example which is illustrated in Fig.1c, the subroutine requires node numbers in the integer double array ELNO(32,6) which provide the description of the focal elements, e.g.

1	0	2	0	9	0
2	0	8	0	9	0
9	0	8	0	13	0

etc.

The calling statement is then

CALL FILL ELNO 6 OR 12 (32,ELNO,6)

for the subroutine to return the following topological description in ELNO(32,6)

1	0	2	8	9	10
2	3	8	13	9	1
9	2	8	14	13	12

etc.

The 0 in this last table signifies that the side 1 2 coincides with the plate boundary. The procedure is similar for the twelve point topologies which are considered in sections 3 and 4.

```
      SUBROUTINE FILL ELNO 6 OR 12(NEL,ELNO,JTYPE)
C • • • • • • • • • • • • • • • • • • • • • • • • • • • • • • • • • • • • • • •
C   NEL = NUMBER OF ELEMENTS.
C  ELNO = INTEGER DOUBLE ARRAY OF NODE NUMBERS TAKEN IN ORDERED
C         SEQUENCE. THE SUBROUTINE MUST BE SUPPLIED WITH AN ELNO WHICH
C         PRESCRIBES THE NODE NUMBERS FOR ONE FOCAL ELEMENT TO EACH ROW
C         OF JTYPE NUMBERS, EACH OF THESE FOCAL NODE NUMBERS IS FOLLOWED
C         BY ZEROS (ONE IF JTYPE=6, THREE IF JTYPE=12).
C JTYPE = PRESCRIBED AS 6 OR 12 TO FILL ELNO 6 OR 12 RESPECTIVELY.
      INTEGER ELNO(NEL,JTYPE),ELROW,ELCOL
C • • • • • • • • • • • • • • • • • • • • • • • • • • • • • • • • • • • • • • •
      INTEGER JOIN(25,4)
C     NOTE: IF THE NUMBER OF ELEMENTS WITH A COMMON NODE EXCEEDS 25
C     THE FIRST DIMENSION OF JOIN MUST BE REDIMENSIONED ACCORDINGLY.
C • • • • • • • • • • • • • • • • • • • • • • • • • • • • • • • • • • • • • • •
      INTEGER IDENT(500)
      DO 1 I=1,500
C     NOTE: IF THE LARGEST NODE NUMBER EXCEEDS 500 THEN THE LAST TWO
C     STATEMENTS MUST BE REDIMENSIONED ACCORDINGLY.
C • • • • • • • • • • • • • • • • • • • • • • • • • • • • • • • • • • • • • • •
    1 IDENT(I)=1
      JK=4
      IF(JTYPE.EQ.6)JK=2
      DO 5 ELROW=1,NEL
      DO 5 ELCOL=1,1+2*JK,JK
      NODE=ELNO(ELROW,ELCOL)
      IF(IDENT(NODE).EQ.0)GO TO 5
      IDENT(NODE)=0
      NJOINS=0
      DO 2 I=ELROW,NEL
      DO 2 J=1,1+2*JK,JK
      IF(ELNO(I,J).NE.NODE)GO TO 2
      NJOINS=NJOINS+1
      JOIN(NJOINS,1)=I
      JOIN(NJOINS,2)=J
      J4=J+JK
      IF(J4.GT.JTYPE)J4=J4-JTYPE
      JOIN(NJOINS,3)=ELNO(I,J4)
      J8=J+2*JK
      IF(J8.GT.JTYPE)J8=J8-JTYPE
      JOIN(NJOINS,4)=ELNO(I,J8)
    2 CONTINUE
      DO 5 K=1,NJOINS
      I=JOIN(K,1)
      N=JOIN(K,2)
      N8=N+2*JK
      IF(N8.GT.JTYPE)N8=N8-JTYPE
      IN4=JOIN(K,3)
      IN8=JOIN(K,4)
      DO 4 KA=1,NJOINS
      IF(K.EQ.KA)GO TO 4
      J3=JOIN(KA,3)
      J4=JOIN(KA,4)
      IF(JTYPE.EQ.6)GO TO 3
      IF(IN4.EQ.J4)ELNO(I,N+2)=J3
      IF(IN8.EQ.J3)ELNO(I,N8+2)=J4
      GO TO 4
    3 IF(IN4.EQ.J4)ELNO(I,N+1)=J3
      IF(IN8.EQ.J3)ELNO(I,N8+1)=J4
    4 CONTINUE
      IF(JTYPE.EQ.6)GO TO 5
      N10=N+10
      IF(N10.GT.JTYPE)N10=N10-JTYPE
      IN2=ELNO(I,N+2)
      IN10=ELNO(I,N10)
      DO 5 KA=1,NJOINS
      IF(K.EQ.KA)GO TO 5
      J3=JOIN(KA,3)
      J4=JOIN(KA,4)
      IF(IN2.EQ.J4)ELNO(I,N+1)=J3
      IF(IN10.EQ.J3)ELNO(I,N10+1)=J4
    5 CONTINUE
      RETURN
      END
```

REFERENCES

No.	Author(s)	Title, etc.
1	R. W. Clough J.L. Tocher	Finite element stiffness matrices for analysis of plates in bending. Proc. Conf. Matrix Methods in Struct. Mech. AFFDL-TR-66-80, 515 (1966)
2	G. P. Bazeley Y. K. Cheung B. M. Irons O. C. Zienkiewicz	Triangular elements in plate bending - conforming and non-conforming solutions. Proc. Conf. Matrix Methods in Struct. Mech., AFFDL-TR-66-80, 547 (1966)
3	L. S. D. Morley B. C. Merrifield	On the conforming cubic triangular element for plate bending. In preparation.
4	K. Bell	Triangular plate bending elements. In: Finite Element Methods in Stress Analysis, edited by Holand and Bell. Tapir, 213 (1969)
5	L. R. Herrmann	Finite-element bending analysis for plates. Jour. Engng. Mech. Div. Am. Soc. Civ. Engrs., 93 EM5, 13 (1967)
6	K. Hellan	Analysis of elastic plates in flexure by a simplified finite element method. Acta Polytechnica Scandinavica. Civ. Engng. Bldg. Constructn. Series, No.46 (1967)
7	D. J. Allman	Triangular finite elements for plate bending with constant and linearly varying bending moments. IUTAM Symp. High-speed Computing Elastic Structures (Liège) (1970)
8	L. S. D. Morley	The constant-moment plate bending element. Jour. Strain Analysis, 6, 20 (1971)
9	T. Fujino	Analyses of hydrodynamic and plate structure problems by finite element methods. Japan - US Semin. Matrix Meth. Struct. Analysis Design, (Tokyo) (1969)
10	J. H. Argyris	Triangular elements with linearly varying strain for the matrix displacement method. Jour. Roy. Aero. Soc., 69, 711 (1965)
11	B. Fraeijs de Veubeke	Displacement and equilibrium methods in the finite element method. In: Stress Analysis, edited by O. C. Zienkiewicz and G. S. Hollister, Wiley, 145 (1965)
12	R. C. J. Howland	On the stresses in the neighbourhood of a circular hole in a strip under tension. Phil. Trans. Roy. Soc. London, A, 229, 49 (1930)
13	H. Hengst	Beitrag Zur Beurteilung des Spannungszustandes einer gelochten Scheibe. Ztschr.f.angew Math.und Mech., 18, 44 (1938)
14	L. S. D. Morley B. C. Merrifield	Bandwidth reduction of label sequences as encountered in finite element calculations. Internal Report of the Royal Aircraft Establishment, Farnborough (1970)